

Enhanced low field magnetoresistive response in $(\text{La}_{2/3}\text{Sr}_{1/3}\text{MnO}_3)_x/(\text{CeO}_2)_{1-x}$ composite thick films prepared by screen printing

S. Valencia, O. Castaño, J. Fontcuberta, B. Martínez, and Ll. Balcells

Citation: *Journal of Applied Physics* **94**, 2524 (2003);

View online: <https://doi.org/10.1063/1.1589174>

View Table of Contents: <http://aip.scitation.org/toc/jap/94/4>

Published by the [American Institute of Physics](#)

Articles you may be interested in

Enhanced field sensitivity close to percolation in magnetoresistive $\text{La}_{2/3}\text{Sr}_{1/3}\text{MnO}_3/\text{CeO}_2$ composites
Applied Physics Letters **74**, 4014 (1999); 10.1063/1.123245

Enhanced tunable magnetoresistance properties over a wide temperature range in epitaxial $(\text{La}_{0.7}\text{Sr}_{0.3}\text{MnO}_3)_{1-x}:(\text{CeO}_2)_x$ nanocomposites
Journal of Applied Physics **118**, 065302 (2015); 10.1063/1.4928160

Magnetotransport properties of quasi-one-dimensionally channeled vertically aligned heteroepitaxial nanomazes
Applied Physics Letters **102**, 093114 (2013); 10.1063/1.4794899

Fabrication of 0-3 type manganite/insulator composites and manipulation of their magnetotransport properties
Journal of Applied Physics **106**, 104317 (2009); 10.1063/1.3262624

Doping of interfaces in $(\text{La}_{0.7}\text{Sr}_{0.3}\text{MnO}_3)_{1-x}:(\text{MgO})_x$ composite films
Applied Physics Letters **81**, 1648 (2002); 10.1063/1.1503849

Effect of magnetic coupling on the magnetoresistive properties in $\text{La}_{0.67}\text{Sr}_{0.33}\text{MnO}_3/\text{BaFe}_{11.3}(\text{ZnSn})_{0.7}\text{O}_{19}$ composites
Journal of Applied Physics **90**, 2924 (2001); 10.1063/1.1392962

Scilight

Sharp, quick summaries illuminating
the latest physics research

Sign up for FREE!



Enhanced low field magnetoresistive response in $(\text{La}_{2/3}\text{Sr}_{1/3}\text{MnO}_3)_x/(\text{CeO}_2)_{1-x}$ composite thick films prepared by screen printing

S. Valencia, O. Castaño, J. Fontcuberta, B. Martínez, and Ll. Balcells^{a)}

Institut de Ciència de Materials de Barcelona CSIC, Campus UAB, Bellaterra 08193, Spain

(Received 21 January 2003; accepted 12 May 2003)

The magnetoresistance and magnetization of $(\text{La}_{2/3}\text{Sr}_{1/3}\text{MnO}_3)_x(\text{LSMO})/(\text{CeO}_2)_{1-x}$ ($0.64 \leq x \leq 1$) composite thick films have been studied as a function of the manganite concentration. It is found that for high LSMO content, when the applied magnetic field is perpendicular to the film plane, the attainable low field magnetoresistance (LFMR) response is drastically reduced due to demagnetizing field effects. These effects are suppressed when the concentration of CeO_2 is increased, thus an enhancement of the LFMR is observed. These results can be very important for developing magnetic sensors working in the low magnetic field regime when magnetic field needs to be applied perpendicular to the film plane. © 2003 American Institute of Physics.

[DOI: 10.1063/1.1589174]

I. INTRODUCTION

Manganese perovskites are a subject of very active research due to the broad range of interesting magnetotransport properties they display, which can be very useful for the development of new magnetic and magnetoresistive devices.^{1,2} Between them $\text{La}_{2/3}\text{Sr}_{1/3}\text{MnO}_3$ (LSMO) is one of the most attractive due to both its high Curie temperature ($T_C \approx 360$ K) and magnetoresistive response,³ making possible the fabrication of devices working at room temperature (RT).² On the other hand, it is also well known that in the low magnetic field (H) regime manganite ceramics have an important extrinsic contribution to the magnetoresistance (MR) known as low field magnetoresistance (LFMR). Two different aspects are implicated in the LFMR, one is the rotation of the magnetization of grains when increasing H and the other is the spin polarized tunneling conduction through grain boundaries (GB).⁴ Therefore, LFMR should be especially important in granular systems⁴⁻⁷ and artificially generated interfaces.⁸ In fact, LFMR responses near 30% have been found in granular systems at low temperatures, but on raising temperature a substantial reduction is observed well below T_C . This reduction is mainly due to the depolarization of the conduction charge carriers because of the scattering generated at magnetically disordered interfaces in GB.^{4,5} Nevertheless, values of the LFMR of technological interest are still attainable close to T_C making granular LSMO samples useful for the design and development of some types of magnetic and magnetoresistive devices working at RT.^{1,2}

With this goal in mind, important efforts have been devoted to improve the LFMR response in granular systems. One of the routes used is the reduction of the conduction path by diluting LSMO powders with a magnetic insulator (MI)^{9,10} or a nonmagnetic insulator (NMI).^{11,12} In fact, LFMR responses obtained in diluted LSMO/NMI compos-

ites have demonstrated to be adequate for some technological applications, such as potentiometers, position sensors, etc.²

From the technological point of view to develop competitive low cost magnetic sensors, based on the LFMR response of manganite materials, involves two different aspects:

- A high enough magnetoresistive response at RT and above is required;
- a cheap and easy-to-implement fabrication technology should be available.

In this work we face these two aspects. We analyze the LFMR response of $(\text{LSMO})_x/(\text{CeO}_2)_{1-x}$ composite thick films as a function of the LSMO content showing that it can be adequate for some applications at RT. On the other hand, we have explored the suitability of the screen-printing technology, already well known and widely used in the field of cheap electronic sensors, to prepare $(\text{LSMO})_x/(\text{CeO}_2)_{1-x}$ thick films suitable for the fabrication of manganite-based sensor.

II. EXPERIMENT

We have prepared a series of $(\text{LSMO})_x/(\text{CeO}_2)_{1-x}$ composite thick films, being x the volume fraction of LSMO, deposited on Al_2O_3 polycrystalline substrates by using the screen-printing technique. The powders have been mixed in the adequate volume ratio with an organic vehicle in a weight ratio of 2/1, and then the mixture was grinded in order to obtain homogeneous printable ink.

The LSMO powder has been prepared by the solid-state reaction technique^{13,14} and grinded for several hours in an attrition system to obtain small particles, well below $0.1 \mu\text{m}$.¹⁵ As a nonmagnetic insulating diluting phase we have chosen CeO_2 because it is an extremely refractory oxide with low reactivity, which will minimize any chemical interdiffu-

^{a)} Author to whom correspondence should be addressed; electronic mail: balcells@icmab.es

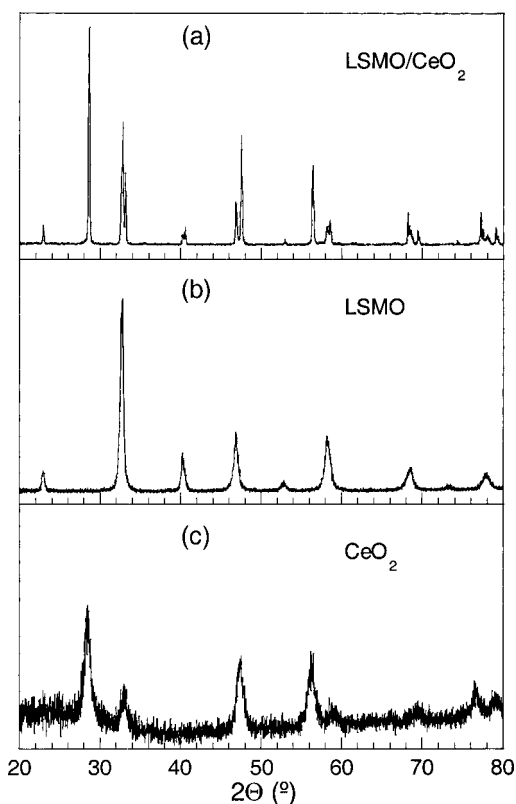


FIG. 1. Θ - 2Θ x-ray diffraction patterns for the original powders [(b) and (c)] and for the thick film with $x=0.73$ (a).

sion with LSMO grains during the sintering process.

In order to obtain particles of similar size to that of LSMO cerium oxide powders has been prepared by the sol-gel technique following the process summarized next. Hydrous ceria was prepared at room temperature by slow addition and stirring of $\text{Ce}(\text{NO}_3)_3 \cdot n\text{H}_2\text{O}$ dissolved in a 5% diluted H_2O_2 aqueous solution of pH adjusted to 10 with ammonia.^{16,17} Finally, the precipitated gel was dried and annealed for 4 h at 600 °C to obtain the cerium oxide. The grain size of LSMO (≈ 25 nm) and CeO_2 (≈ 10 nm) powders has been independently evaluated from x-ray diffraction data by using the Scherrer method.

Thick films were printed on Al_2O_3 polycrystalline substrates and then sintered in air at 1200 °C for 10 min in order to evaporate the organic vehicle (below 450 °C) and to achieve good adherence to the substrate and good electrical conductivity between grains (see Ref. 2 for details). X-ray diffraction data (see Fig. 1) do not show any traces of impurities in the films after sintering in agreement with previously reported results.¹¹ Therefore, indicating that interdiffusion between LSMO and CeO_2 during the sintering process is negligible. The microstructure and thickness of the films have been determined by using scanning electron microscopy (SEM). A similar thickness (~ 20 μm) has been found for all the samples [Fig. 2(a)]. On the other hand, thick films present a homogenous mixture of both LSMO and CeO_2 components with a mean grain size well below 1 μm [see Fig. 2(b)]. Nevertheless some large precipitates of CeO_2 (~ 50 μm) can be detected thus, modifying the effective ratio between the metallic and the insulating components in the

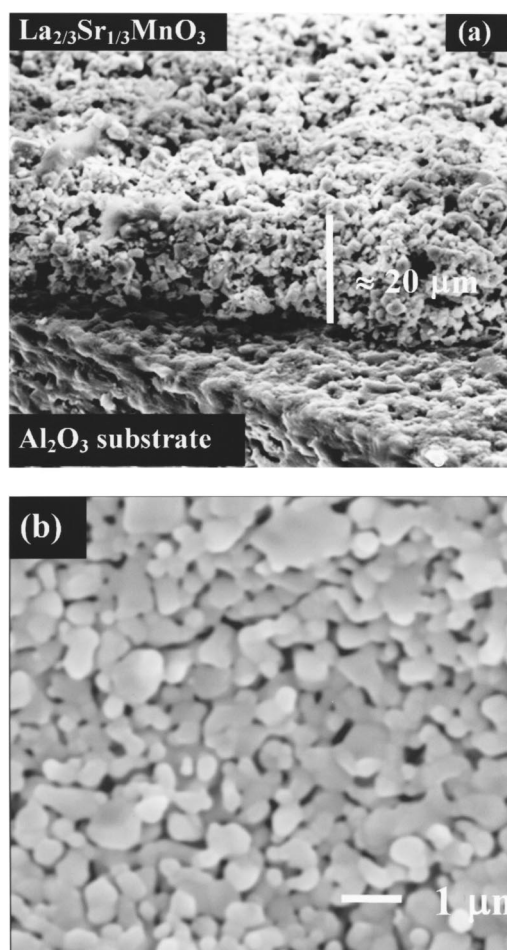


FIG. 2. SEM images of two films: (a) Section of a 100% LSMO ($x=1$) film of about 20 μm thick; (b) surface of an $x=0.81$ film.

matrix where the conduction take place. The actual ratio of both components in the matrix, excluding large precipitates of CeO_2 , has been determined by EDX analysis. The actual concentration of LSMO (x) of the samples reported in this work is 100%, 95%, 89%, 81%, 73%, and 64% in volume. For lower concentration of LSMO the transport properties of the films were not measurable due to their very high resistance, and thus will not be further considered.

The RT magnetic properties have studied by using a commercial QD-SQUID magnetometer with the magnetic field applied parallel and perpendicular to the film plane. The magnetotransport properties have also been measured at RT, in samples with typical dimensions of about 2×1 mm², by using the four-probe method in a homemade experimental setup.

III. RESULTS AND DISCUSSION

The RT magnetization curves of samples with compositions $x=1$ and $x=0.64$ are depicted in Fig. 3. Comparing the curves obtained with the field applied parallel (H_{\parallel}) and perpendicular (H_{\perp}) to the film plane, it is evident from the figure that for the sample with $x=1$ (LSMO only) the magnetic moment lies in the film plane. In the perpendicular-to-plane geometry a larger field is required to reach technical saturation of the magnetization due to the high demagnetiz-

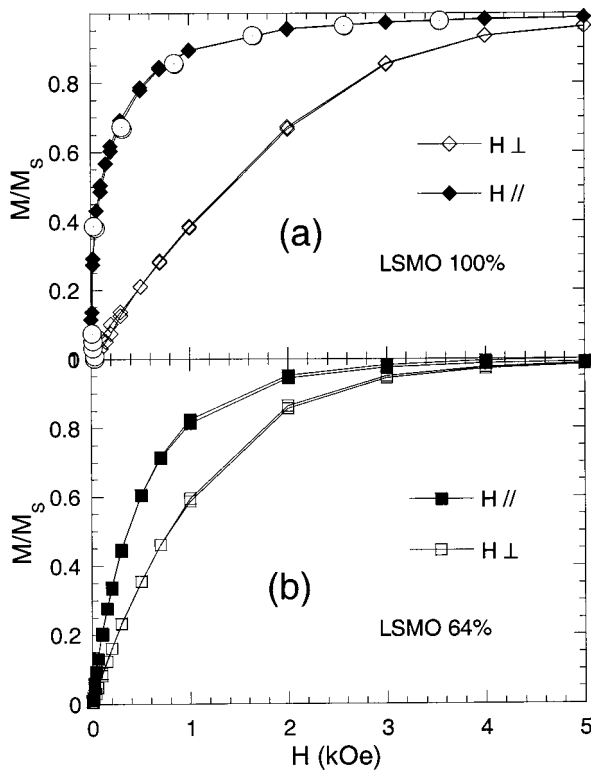


FIG. 3. RT magnetization curves with the magnetic field applied parallel (H_{\parallel}) (full symbols) and perpendicular (H_{\perp}) (open symbols) to the film plane: (a) $x=1$ sample (b) $x=0.64$ sample. Open circles in (a) correspond to the H_{\perp} geometry after correction for demagnetizing field effects.

ing field existing in this geometry. The value of the demagnetizing factor ($\eta \sim 4.2, H_D = \eta M$) has been determined by comparing magnetization curves measured in both H_{\parallel} and H_{\perp} geometries. In the case of the sample with $x=0.64$ differences between H_{\parallel} and H_{\perp} magnetization curves are rather small [see Fig. 3(b)] which implies a much smaller demagnetizing field.

These observations indicate that as the concentration of LSMO decreases mean distances between LSMO grains increase and exchange coupling between grains is reduced giving place to the formation of FM clusters, thus shape anisotropy and consequently the demagnetizing field, are drastically reduced. This effect is clearly evidenced in the sample with $x=0.64$ [Fig. 3(b)]. Therefore in the limit of noninteracting particle we expect to obtain the same curve for both directions, corresponding to the magnetization of isolated LSMO grains. That means that the demagnetizing field associated to the H_{\perp} geometry has vanished. On the other hand, at RT the remanence and the coercive field are almost negligible as expected for a quite soft magnetic material, such as LSMO, measured close to the Curie temperature ($\sim 0.8T_C$).

We move now to comment on the magnetotransport data. The RT conductivity for several thick films with different LSMO concentrations (x) is shown in Fig. 4. It is found that the conductivity, G , decrease as $G \propto e^{-x}$, as typically found in other percolating systems.¹⁸ The RT magnetoresistance of the sample with $x=1$ and in the H_{\parallel} geometry is shown in Fig. 5. It is worth pointing out that a clear variation of the value of

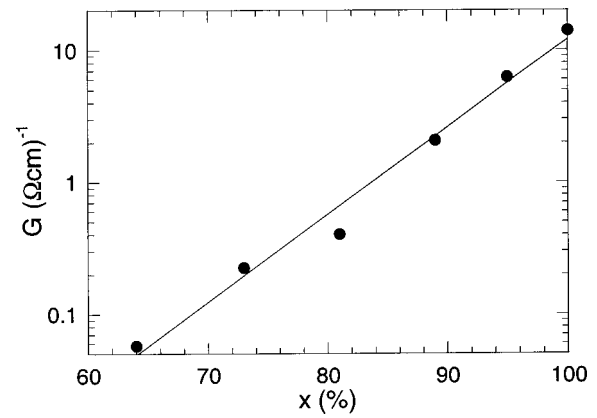


FIG. 4. Conductivity of different samples as a function of x .

the LFMR is observed depending on the direction of the measuring current with respect to the magnetic field (parallel or perpendicular to the field). The change observed is due to the well-known anisotropic magnetoresistance (AMR) and at RT amounts about 0.3% in agreement with previous results reported both in thin¹⁹ and thick films.²⁰

On the other hand, a more relevant change of the RT magnetoresistance is found depending on the direction of the applied field with respect to the film plane (see Fig. 6). Depending on the experimental geometry, H_{\parallel} or H_{\perp} , a large reduction of the MR is detected. We should mention here that in these experiments the measuring current and the magnetic field were always perpendicular to each other to keep constant the AMR contribution. Under these circumstances, having in mind the magnetic behavior of the samples (see Fig. 3) we attribute the observed differences basically to shape anisotropy. The reduction of the LFMR observed in the H_{\perp} geometry can be explained by taking into account demagnetizing field effects. This is also illustrated in Fig. 6 where values of MR corresponding to H_{\perp} geometry after correction for demagnetizing field effects (open circles) are shown to coincide with those of the H_{\parallel} geometry. Therefore, after taking into account demagnetizing field effects (see Fig. 3) the

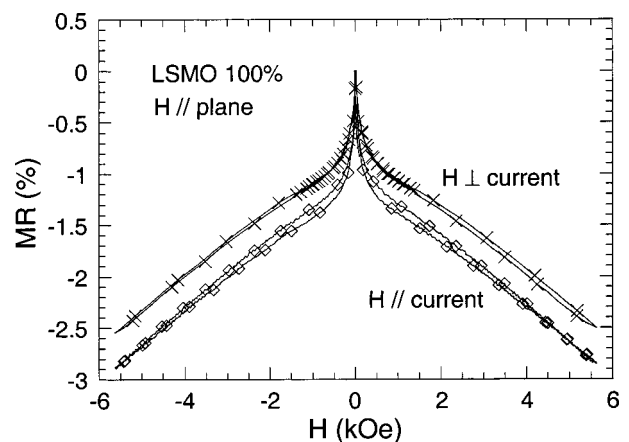


FIG. 5. Room temperature MR of the $x=1$ sample, measured with the applied field, H , parallel to the film plane, as a function of the direction of the measuring current, i.e., parallel and perpendicular to the magnetic field.

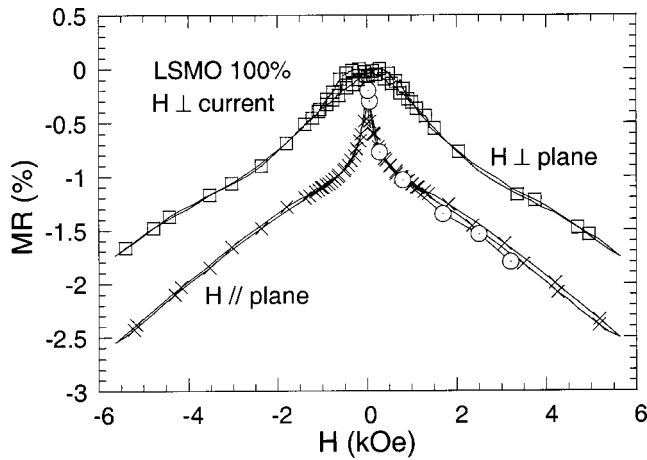


FIG. 6. Room temperature MR of the $x=1$ sample measured with the applied field, H , parallel and perpendicular to the film plane. The symbols (\odot) correspond to experimental values obtained in the H perpendicular-to-plane geometry after correction for demagnetizing field effects.

observed differences between the MR response in the H_{\parallel} and H_{\perp} geometries disappear (see Fig. 6).

The observed dependence of the MR as a function of the LSMO concentration also points in this direction (see Fig. 7). In the H_{\perp} geometry an important change of the LFMR as a function of x is detected [Fig. 7(a)]. It is evident from the figure that the demagnetizing field plays an important role

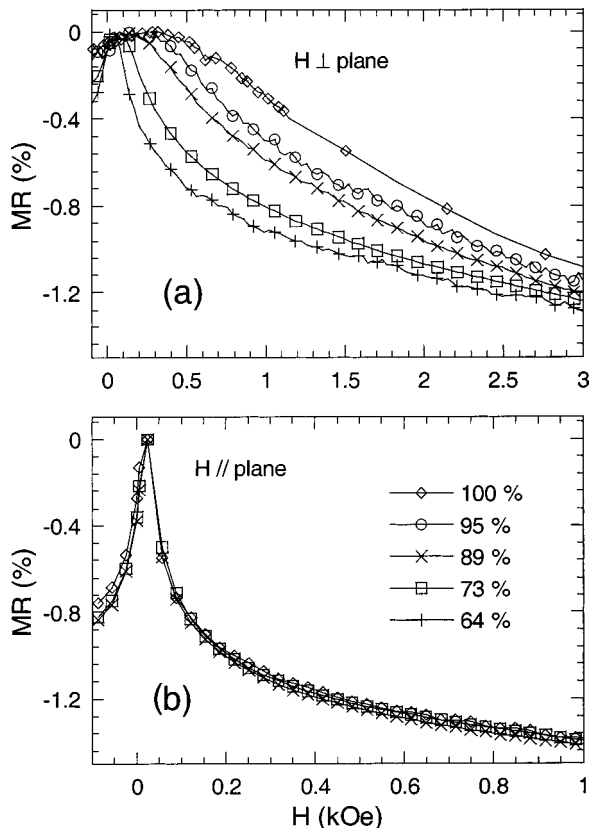


FIG. 7. Room temperature MR for samples with different LSMO contents with the magnetic field, H , applied perpendicular (a) and parallel (b) to the film plane. The measuring current was always perpendicular to the magnetic field.

for high LSMO concentration but progressively vanish as x decreases. As previously described when we discussed the magnetic properties of the samples, for high concentrations of LSMO magnetic interactions between grains are strong enough and therefore the samples behave as a uniform magnetized system with a large demagnetizing field. In diluted samples, the magnetic grains are further apart and intergranular magnetic interactions become weaker as x decreases. The system behaves like a cluster system and therefore, shape anisotropy decrease and the demagnetizing field is drastically reduced giving place to an important enhancement of the LFMR. On the contrary in the H_{\parallel} geometry, the demagnetizing factor is almost zero, and no appreciable differences in MR curves as a function of x are found [see Fig. 6(b)].

Nevertheless, we should mention that magnetization curves do show some clear differences as a function of the LSMO concentration (see Fig. 3). Therefore, these results make evident that the microstructure should also play a role on the magnetotransport properties since MR appears mainly at the interfaces between magnetic particles.

IV. CONCLUSIONS

In summary, we have prepared thick films of LSMO/CeO₂ composites [with different LSMO concentration rates (x)] by using the screen printing technique. The sintered films present good adherence and good connectivity between grains making evident the suitability of the screen-printing technique for the fabrication of some manganite-based magnetoresistive devices. We have studied their magnetic and transport properties as a function of the LSMO content at room temperature. In films with high concentration of LSMO, i.e., strong magnetic coupling between grains, shape anisotropy effects generate an important demagnetizing field. As dilution increases, magnetic coupling between grains decreases and the film behaves more like a system of separated magnetic clusters. Therefore, for high LSMO concentration, when the applied magnetic field is perpendicular to the film plane, the attainable LFMR response is reduced due to demagnetizing field effects. This effect is suppressed when the concentration of CeO₂ is increased, thus an enhancement of the LFMR is observed. Even though the LFMR values is lower than that obtained when the magnetic field is applied parallel to the film plane.

These results are very important for developing magnetic sensors working in the low magnetic field regime when magnetic field needs to be applied perpendicular to the film plane. The observed increase of MR in the H_{\perp} geometry in concomitance with the dilution of the MR material with an isolating compound can be of great interest in order to improve the sensitivity of magnetic devices based on these ceramic materials.

ACKNOWLEDGMENTS

This work has been supported by the CICYT (MAT99-0984 and MAT2000-1290-C03-03), and the Generalitat de Catalunya (GRQ99-8029).

- ¹Y. Lu, W. Li, G. Gong, G. Xiao, A. Gupta, P. Lecoeur, J. Sun, Y. Wang, and V. Dravid, *Phys. Rev. B* **54**, R8357 (1996); M. Viret, M. Drouet, J. Nassar, J. P. Contour, C. Fermon, and A. Fert, *Europhys. Lett.* **39**, 545 (1997).
- ²Ll. Balcells, J. Cifre, A. Calleja, and J. Fontcuberta, *Sens. Actuators A* **81**, 64 (2000); Ll. Balcells, R. Enrich, J. Mora, A. Calleja, J. Fontcuberta, B. Martínez, and X. Obradors, *Appl. Phys. Lett.* **69**, 1486 (1996).
- ³S. Jin, T. H. Tiefel, M. McCormack, R. A. Pastnacht, R. Ramesh, and L. H. Chen, *Science* **264**, 463 (1994).
- ⁴H. Y. Hwang, S.-W. Cheong, N. O. Ong, and B. Batlogg, *Phys. Rev. Lett.* **77**, 2041 (1996).
- ⁵Ll. Balcells, J. Fontcuberta, B. Martínez, and X. Obradors, *J. Phys.: Condens. Matter* **10**, 1883 (1998).
- ⁶R. Mahesh, R. Mahendrian, A. K. Raychaudhuri, and C. N. Rao, *Appl. Phys. Lett.* **68**, 2291 (1996).
- ⁷R. D. Sánchez, J. Rivas, C. Vázquez-Vázquez, A. López-Quintela, M. T. Causa, M. Tovar, and S. Oseroff, *Appl. Phys. Lett.* **68**, 1 (1996).
- ⁸N. D. Mathur, G. Burnell, S. P. Isaac, T. J. Jackson, B.-S. Teo, J. L. MacManus-Driscoll, L. F. Cohen, J. E. Evetts, and M. G. Blamire, *Nature (London)* **387**, 266 (1997).
- ⁹C.-H. Yan, Z.-G. Xu, T. Zhu, Z.-M. Wang, F.-X. Cheng, Y.-H. Huang, and C.-S. Liao, *J. Appl. Phys.* **87**, 5588 (2000).
- ¹⁰Q. Huang, J. Li, X. J. Huang, C. K. Ong, and X. S. Gao, *J. Appl. Phys.* **90**, 2924 (2001).
- ¹¹Ll. Balcells, A. E. Carrillo, B. Martínez, and J. Fontcuberta, *Appl. Phys. Lett.* **74**, 4014 (1999).
- ¹²D. K. Petrov, L. Krusin-Elbaum, J. Z. Sun, C. Feild, and P. R. Duncombe, *Appl. Phys. Lett.* **75**, 995 (1999).
- ¹³J. Fontcuberta, B. Martínez, A. Seffar, S. Piñol, J. L. Garcia-Muñoz, and X. Obradors, *Europhys. Lett.* **34**, 379 (1996).
- ¹⁴J. Fontcuberta, B. Martínez, A. Seffar, S. Piñol, A. Roig, E. Molins, X. Obradors, J. Alonso, and J. M. Gonzalez-Calbet, *J. Appl. Phys.* **79**, 5182 (1996).
- ¹⁵Ll. Balcells, J. Fontcuberta, B. Martínez, and X. Obradors, *Phys. Rev. B* **58**, R14697 (1998).
- ¹⁶B. Djuričić and S. Pickering, *J. Eur. Ceram. Soc.* **19**, 1925 (1999).
- ¹⁷L. Mestres, M. L. Martínez-Sarrión, O. Castaño, and J. Fernández-Urban, *Z. Anorg. Chem.* **627**, 294 (2001).
- ¹⁸D. K. Petrov, L. Krusin-Elbaum, J. Z. Sun, C. Feild, and P. R. Duncombe, *Appl. Phys. Lett.* **75**, 995 (1999).
- ¹⁹M. Ziese and S. P. Sena, *J. Phys.: Condens. Matter* **10**, 2727 (1998).
- ²⁰Ll. Balcells, E. Calvo, and J. Fontcuberta, *J. Magn. Magn. Mater.* **242–245**, 1166 (2002).